Title
Characterization and structural analysis of twinned La2−xSrxCuO4±δ crystals by neutron diffraction

Journal
Physica C Superconductivity, 191(3-4)

ISSN
0921-4534

Authors
Braden, M
Heger, G
Schweiss, P
et al.

Publication Date
1992-02-01

DOI
10.1016/0921-4534(92)90944-8

Physica C 191 (1992) 455–468
North-Holland

PHYSICA C

Characterization and structural analysis of twinned $La_{2-x}Sr_xCuO_{4\pm\delta}$ crystals by neutron diffraction

M. Braden [a,b], G. Heger [a], P. Schweiss [a,c], Z. Fisk [d], K. Gamayunov [e], I. Tanaka [f] and H. Kojima [f]

[a] *Laboratoire Léon Brillouin (CEA-CNRS), 91191 Gif sur Yvette Cedex, France*
[b] *II. Physikalisches Institut der Universität Köln, Zülpicher Str. 77, 5000 Köln 41, Germany*
[c] *Kernforschungszentrum Karlsruhe, Institut für Nukleare Festkörperphysik, Postfach 3640, 7500 Karlsruhe, Germany*
[d] *Los Alamos National Laboratory, Los Alamos, NM87545, USA*
[e] *Institute of General Physics, 182 Moscow, USSR*
[f] *Institute of Inorganic Synthesis, Yamanashi University, Miyamae 7, Kofu 400, Japan*

Received 6 December 1991

The microstructure of $La_{2-x}Sr_xCuO_{4\pm\delta}$ crystals has been studied by neutron diffraction. Profile analysis of the intensity of Bragg reflections shows that the large crystals consist of domains of four different orientations, which are related to the symmetry reduction of the phase transition I4/mmm–Abma. The domain structure has a strong influence on the extinction, therefore it may be studied macroscopically. The microstructure is formed at the phase transition and does not change in the orthorhombic phase. After a first cooling cycle the formation of the domains appears to be reversible without a temperature hysteresis. The same domain structure appears in consecutive cooling cycles. This indicates a pinning of the domain structure by lattice defects. A data set of Bragg reflection intensities obtained on a twinned $La_{1.93}Sr_{0.07}CuO_4$ crystal at room temperature could be refined with special consideration of the microtwinning. The achieved precision of structural parameters is almost comparable to structural analyses on monodomain single crystals.

1. Introduction

The system $(La/RE)_{2-x}M_xCuO_{4\pm\delta}$ (RE=rare earth, M=Sr, Ba) contains a number of structurally different phases whose stabilities depend on the incorporated RE metal and on the earth alkali substitution as well as on the oxygen stoichiometry. At high temperatures pure La_2CuO_4 crystallizes in a tetragonal structure (HTT) of K_2NiF_4 type. The stability of this phase can be discussed with reference to the tolerance factor between the bond lengths of the Cu–O and La/RE/M–O polyhedra [1]. The La–O and Cu–O bond lengths show an increasing mismatch on cooling due to their different thermal expansion. The first response of the system to this mismatch is a strong Jahn–Teller distortion of the CuO_6 octahedra, which are elongated in the *c*-direction, thereby shifting the apical oxygen closer to the La/RE/M sites. This is different in the case of the Jahn–Teller distorted structure of K_2CuF_4 (also of K_2NiF_4 type), where the CuF_6 octahedra are elongated in the *a*, *b* plane causing an antiferrodistortive ordering [2].

An increasing misfit leads to a structural phase transition at T_{T-O} into the low temperature orthorhombic (LTO) polymorph [3]. At the HTT–LTO phase transition the octahedra are tilted around the [0 1 0] or [1 0 0] axis, thereby lowering the space group symmetry to Abma or Bmab. (We use the nonconventional settings F4/mmm instead of I4/mmm for the HTT phase and Abma or Bmab instead of Cmca for the LTO phase. This has the advantage that the unit cell does not change during the phase transition and the long axis is always the *c*-axis.) In undoped La_2CuO_4 the temperature of the phase transition T_{T-O} is about 530 K, but it is very sensitive to the oxygen concentration [4,5]. A substitution of the trivalent La ion by the divalent ions Sr or Ba decreases the orthorhombic distortion rapidly and stabilizes the tetragonal phase [6]. The superconducting compound $La_{1.85}Sr_{.15}CuO_4$ is tetragonal at room

temperature; the transition occurs at about $T_{T-O}=200$ K [7–9]. An additional phase transition has been reported for $La_{2-x}Ba_xCuO_4$ [10,11], where the LTO modification transforms into a low temperature tetragonal (LTT) structure. Two further structural modifications exist in the mixed system $(La/RE)_{2-x}M_xCuO_4$, commonly called T' and T* [12,13]. They are both tetragonal at room temperature and become superconducting by doping with electrons and holes, respectively. It is supposed that at least the T'structure is distorted if smaller RE ions are incorporated [14]. It has been shown that subtle structural changes can destroy the conditions for superconductivity almost completely (for $La_{2-x}Ba_xCuO_4$ see refs. [9,10] and for $La_{2-x-y}Nd_ySr_xCuO_4$ ref. [15]). Furthermore, the HTT–LTO transition is connected to a softening of an optical zone boundary phonon, which may be important to enhance the superconducting T_c in these compounds [16,17]. It therefore seems to be very important for the understanding of superconductivity to obtain as much structural information as possible about the $La_{2-x}Sr_xCuO_{4\pm\delta}$ compounds in general and on details of the HTT–LTO transition in particular.

Unfortunately a detailed structure analysis using single crystals is difficult in the orthorhombic phase due to twinning. The symmetry reduction at the phase transition leads to the occurrence of twin domains corresponding to the two different tilt axes [1 0 0] and [0 1 0] for the CuO_6 octahedra. Strain can influence the size distribution of these domains [18], but without a special treatment the large crystals consist of a multitude of domains. If the domain sizes are large compared to the coherence length of the radiation, there is an incoherent intensity superposition of the Bragg reflections of different twin domains. The diffraction pattern of such a microtwinned crystal is quite similar to one of a tetragonal crystal. Due to the small orthorhombic distortion the angular separation of reflections from different oriented domains may be very small. In this paper we describe the characterization of the microstructure of such crystals, as it is observed by neutron diffraction. We will show that detailed structure analyses carried out on twinned crystals yield results comparable to those of true single crystals. Furthermore, a characterization of large $La_{2-x}Sr_xCuO_{4\pm\delta}$ crystals seems to be valuable as such crystals are increasingly used in recent research.

2. Experimental

We studied several $La_{2-x}Sr_xCuO_{4\pm\delta}$ crystals of various compositions from different laboratories (table 1). The details of the preparation are given in refs. [19] and [20]. Due to doping with Sr^{2+} or excess oxygen the examined crystals are examples for the different physical features in this system, ranging from a strong antiferromagnetic insulator La_2CuO_4 to samples with reduced T_N or spin glass behaviour to superconducting ones. Further data characterizing the samples are given in table 1.

The present neutron diffraction experiments have been performed at the Laboratoire Léon Brillouin in Saclay (France). We used the four-circle diffractometer P 110 which is installed at the hot source (5C.2: $\lambda=0.833$ Å) of the ORPHEE reactor. Initially, the samples, having volumes of 10–60 mm^3, were tested for their suitability, especially with regard to their compositional homogeneousness and for the presence of misoriented parts.

The proposed twinning mechanism discussed below leaves the c-axis invariant, as it is caused by the orthorhombic splitting. Therefore we examined reflections in the reciprocal a^*, b^* plane (mostly (2 2 0), (4 4 0), and (4 0 0)) in ω-scan mode. For these scans the crystals were oriented with the c-axis perpendicular to the diffraction plane. In this orientation the ω-mode rotates the crystal around its c-axis thereby giving the condition for maximum angular separation. That the twinning has no influence on the c-direction was checked by further ω-scans on (0 0 1) reflections.

For the crystal structure analysis the crystal was mounted with its c-axis parallel to the ϕ-axis of the 4-circle diffractometer. This mounting assures a complete intensity integration of the $(h\,k\,0)$ reflections for the ω-scans in bisecting mode. Due to the low χ-resolution the integration is also complete for $(h\,k\,l)$ with $l\neq 0$. Furthermore, this mounting avoids the platelike twin domains to be oriented parallel to the diffraction plane. This would cause anomalous extinction as discussed below. For $(0\,0\,l)$ reflections problems related to the anomalous extinction can be

Table 1
Preparation conditions, Néel temperatures, and superconducting properties of the crystals used in this work (the relative oxygen contents of the two undoped crystals is estimated due to the difference of their T_N and ref. [4])

	La_2CuO_4	$La_2CuO_{4.005}$	$La_{1.93}Sr_{.07}CuO_4$	$La_{1.85}Sr_{.13}CuO_4$
Preparation	Los Alamos National Laboratory, Los Alamos, USA	Los Alamos National Laboratory Los Alamos, USA	Institute of General Physics, Moscow, USSR	Institute of Inorganic Synthesis, Kofu, Japan
Method	flux growth	flux growth and additional annealing in O_2	flux growth and additional annealing in O_2	travelling floating zone
Antiferromagn.	$T_N=296(1)$ K	$T_N=252(1)$ K	-	-
T_{T-O}	~530 K	~500 K	~400 K	196.5(9) K
Superconductivity	-	- traces $T_{conset}=34(1)$ K	$T_c\sim 15$ K large trans. width	$T_c=32.5$ K small trans. width anomaly in c_p

avoided by the Ψ-scan technique. In using the "tetragonal" orientation matrix the intensity integration is optimized for the 2θ splitting. With a wavelength of 0.833 Å and an orthorhombic strain of $\epsilon=(a-b)/(a+b)\sim 0.2\%$ the separation in 2θ was always small compared to the chosen diffractometer resolution, leading to a complete intensity integration also in the longitudinal direction.

We first centered a set of 44 reflections, which are also allowed in the tetragonal high symmetry phase. For this purpose the scan widths were choosen sufficiently large to ensure that the resulting centered positions corresponded well to the center of the multipeak intensity distribution in reciprocal space. This procedure yielded tetragonal cell parameters of the averaged tetragonal structure. The corresponding orientation matrix was then used for the data collection. In order to determine the orthorhombic lattice parameters we further centered a set of reflections which are extinct in Bmab ($h+l=$odd) and a set of reflections extinct in Abma ($k+l=$odd). The final lattice parameters used in the refinement were obtained with a triple axis spectrometer (G4.3, $\lambda=2.36$ Å) and are presented in table 2. These values are consistent with the powder measurements of Takagi et al. for the composition $La_{1.93}Sr_{0.07}CuO_4$ [21].

A complete set of Bragg reflection intensities was obtained for the $La_{1.93}Sr_{0.07}CuO_4$ crystal at room temperature in a halfsphere of reciprocal space up to $2\theta=100°$ corresponding to $(\sin\theta)/(\lambda)\leq 0.92$ Å^{-1}.

Table 2
Lattice parameters, reliability values and structural parameters obtained on the $La_{1.93}Sr_{0.07}CuO_4$ crystal at 295K; a, b, c (Abma) 5.376(2), 5.354(2), 13.186(5) Å; $R_w(F^2)$, $R(F^2)$ 0.0175, 0.0183; twinning ratio α 50.8%

La	x, y, z	0.00446(6), 0.0, 0.36108(3)
	U_{11}, U_{22}, U_{33}	0.00676(7), $=U_{11}$, 0.00392(7)
	U_{13}	0.00028(8)
Cu	U_{11}, U_{22}, U_{33}	0.00361(8), $=U_{11}$, 0.00842(11)
	U_{13}	−0.00025(12)
O(1)	x, y, z	0.25, 0.25, 0.00469(4)
	U_{11}, U_{22}, U_{33}	0.00638(6), $=U_{11}$, 0.01444(11)
	U_{12}	−0.00213(6)
O(2)	x, y, z	−0.02233(13), 0.0, 0.18281(3)
	U_{11}, U_{22}, U_{33}	0.0176(3), 0.0221(4), 0.00663(12)
	U_{13}	−0.00088(14)

In this experiment the orthorhombic splitting is too small for a separation of the reflections from differently oriented domains. Therefore, the collected integrated intensities are always the sum of the four twin contributions.

3. Results and discussion

3.1. Characterization of the microstructure

If a $La_{2-x}Sr_xCuO_{4\pm\delta}$ crystal is cooled through the HTT–LTO phase transition there are possibilities to distort the tetragonal structure. These arise through

the rotation of the CuO_6 octahedra around [1 0 0] or [0 1 0] with a positive or negative sense of rotation. The resulting twin orientations are related to the symmetry reduction during the phase transition [22]. In our case, the (1 1 0) mirror plane of the tetragonal phase is lost by the distortion. In a macroscopic way it can be conserved by the formation of twin domains due to a (1 1 0) mirror plane twin law.

The arrangement of the atomic sites in the CuO_2 plane at an idealized boundary is displayed in fig. 1(a). The same type of domain boundary can be formed at the (1 −1 0) plane. So the entire crystal in the LTO phase consists in general of two sets of two twin orientations sharing either the (1 1 0) or (1 −1 0) plane. Connected to the loss of the (1 1 0) mirror plane the four-fold tetragonal axis is reduced to a two-fold one, but it is just the four-fold rotation which relates the (1 1 0) and (1 −1 0) mirror planes and therefore the two sets of twins. All the resulting twin orientations can be described using either space group Abma or Bmab. Keeping the crystallographic basis with the *a*, *b*- and *c*-axes of the HTT modification the orthorhombic distortion leads to space group Abma when the displacement of the O(2) is parallel to the *a*-axis (rotation around [0 1 0] axis and $a>b$), and to Bmab if the corresponding displacement is parallel to the *b*-axis (rotation around [1 0 0] and $b>a$). A pair of twins with a common plane (1 1 0) or (1 −1 0) plane must contain one

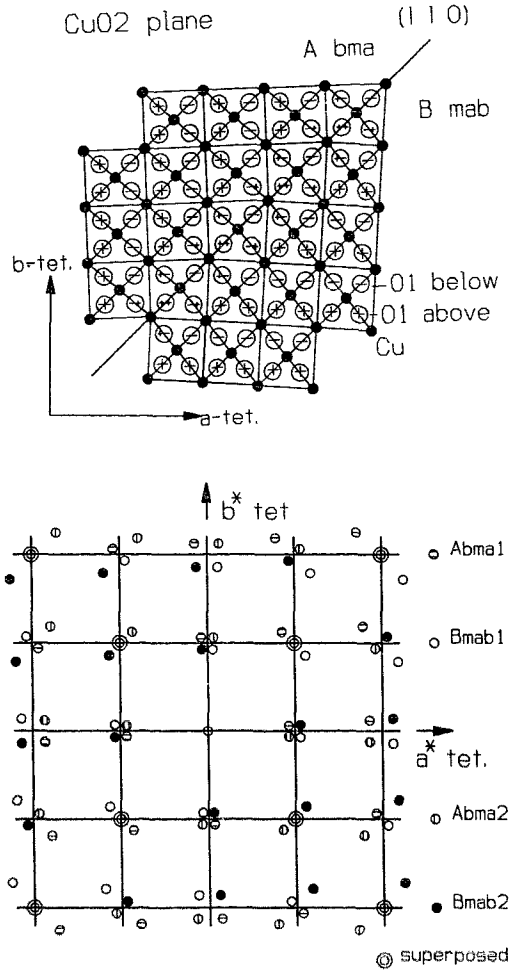

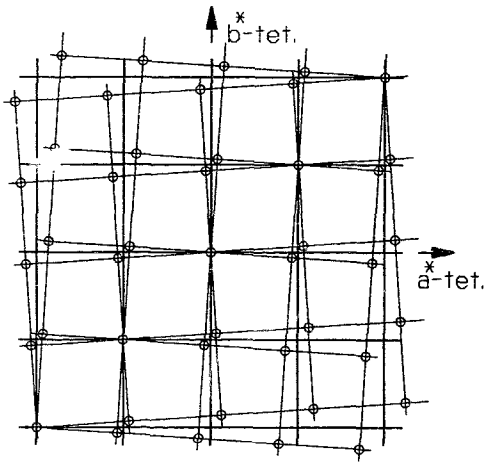

Fig. 1. (a) Arrangement of the atom sites in the CuO_2 plane at a (1 1 0) twin boundary. Due to the orthorhombic distortion the O(1) sites are displaced above (+) and below (−) the Cu plane; near to the boundary the influence of both neighbouring domains is indicated by double signs. (b) Reciprocal space of two domains which are connected by a twin boundary as displayed in fig. (a). (c) Reciprocal space of the superposition of the four different twin orientations.

Abma and one Bmab domain. So we find four different twin orientations $Abma_1$, $Bmab_1$ for the first set and $Abma_2$, $Bmab_2$ for the second set respectively. The tilting angle between the different lattices results from the orthorhombic distortion by (fig. 1(a))

$$\Delta = 90° - 2\arctan(b/a) . \quad (1)$$

The displacements of the oxygens in the orthorhombic structure (indicated by + and − signs in fig. 1(a)) form a puckered arrangement of rows of low and high lying O-chains. At the boundary these chains are turned by $(90 \pm \Delta)°$. The displacements of the oxygen sites in the domain walls result from a superposition of the two orthorhombic domains, as is indicated in fig. 1(a) by two signs. There are oxygen sites where the two influences are in competition (+ −) and others where they are parallel (+ + and − −). It is worth noting that the superimposed displacements of the sites in the boundary (according to fig. 1(a)) are similar to those in space group $P4_2/ncm$ which is the proposed space group of the low temperature phase of $La_{2-x}Ba_xCuO_4$ [10,11]. In a more realistic picture the rotation axis of the CuO_6 tilt may change continously from [0 1 0] in the Abma oriented part via [1 1 0] in the domain wall to [1 0 0] in the Bmab oriented part.

In diffraction experiments on twinned single crystals one observes the superposition of diffraction patterns of the different twin domains. If we assume that the size of the single domains is sufficiently larger than the coherence length of the radiation this superposition is incoherent. One pair of twin domains having (1 1 0) as a common plane($Abma_1$ and $Bmab_1$) corresponds to a reciprocal space which is displayed in fig. 1(b). The reciprocal lattice points $(h\,h\,l)$ are not split, whereas the $(h\,-h\,l)$ are split into two positions, symmetrically with respect to the HTT positions. The reciprocal lattice containing all superposed contributions is the sum of fig. 1(b) and fig. 1(b) rotated by 90°, as it is shown in fig. 1(c).

The superposition of these four different domain orientations causes the multi-peak intensity profiles of Bragg reflections. An ω-scan of a $(h\,h\,0)$ reflection with the c-axis perpendicular to the diffraction plane shows a triple peak structure. The central peak which represents the contributions of two domain orientations has normally the highest intensity. The intensity ratio will amount to 1:2:1 if the volume fractions of the different orientations $Abma_1$, $Abma_2$, $Bmab_1$ and $Bmab_2$ are equal. For the $(h\,0\,0)$ reflections Abma and Bmab contributions are separated (fig. 1(c)) by different 2Θ angles. With a limited $\Delta\lambda/\lambda$ resolution of about 1% on the four-circle diffractometer this 2Θ splitting is barely observable. Furthermore, two domains of the same type are tilted by the angle Δ, which can be measured by ω-scans. For arbitrary reflections the situation becomes more complicated. There is always a superposition of the contributions from the four domain orientations, but as the scan direction is not optimized for observation of the splitting the resulting intensity profiles can become complicated [23].

In fig. 2 we present reflection profiles for the undoped crystal whose composition is close to La_2CuO_4. The full width at half maximum (FWHM) of the (0 0 14) reflection of 0.20(3)° correspond to the 2Θ-dependent diffractometer resolution in this configuration. In this way the mosaic spread of the c direction can be estimated to be lower than 0.03°, and the stacking of the CuO planes seems to be almost perfect. But the profiles of (2 2 0) and (0 4 0) reflections clearly show the twinning. For (0 4 0) we see the expected superposition of two peaks, and for (2 2 0) there is a central peak with two satellites, which show each half the intensity of the central component. Equivalent results are obtained for the (2 0 0) and (4 4 0) reflections. These observed intensity profiles are in perfect agreement with the presented scheme. Fits of the profiles with two or three Gaussian distributions for all reflections confirmed that the FWHM of the different contributions are almost identical and only enlarged by 0.07(2)° with respect to the diffractometer resolution. The angular splitting of the two peaks at (0 4 0), 0.52 (3)° and that of the two satellites at (2 2 0), 0.54(5)° are in good agreement with each other. For the second $La_2CuO_{4.005}$ crystal examined (fig. 3), we find nearly the same reflection profiles. In this crystal too the mosaicity of the c-direction is quite low (0.04(4)°). Again the intensity profiles of the $(h\,k\,0)$ reflections can be fitted with a superposition of two or three Gaussian distributions resulting in peakwidths which are 0.10(3)° larger than the resolution, and a splitting angle of 0.50(4)°. But the intensity ratios are quite different for this crystal. For (2 −2 0), the

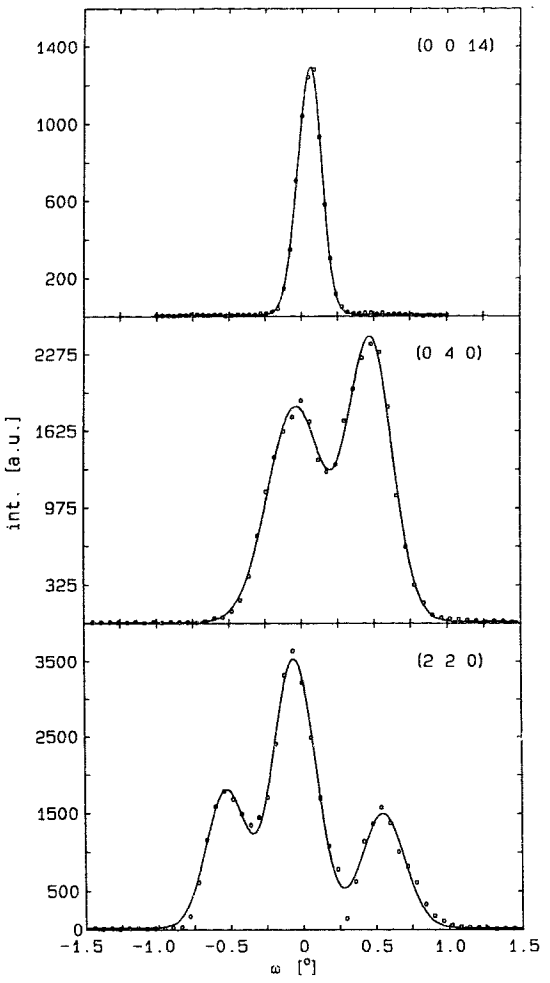

Fig. 2. Intensity profiles of the (0014), (040), and (220) Bragg reflections of the La_2CuO_4 crystal in the ω-scan mode with the c-axis perpendicular to the diffraction plane.

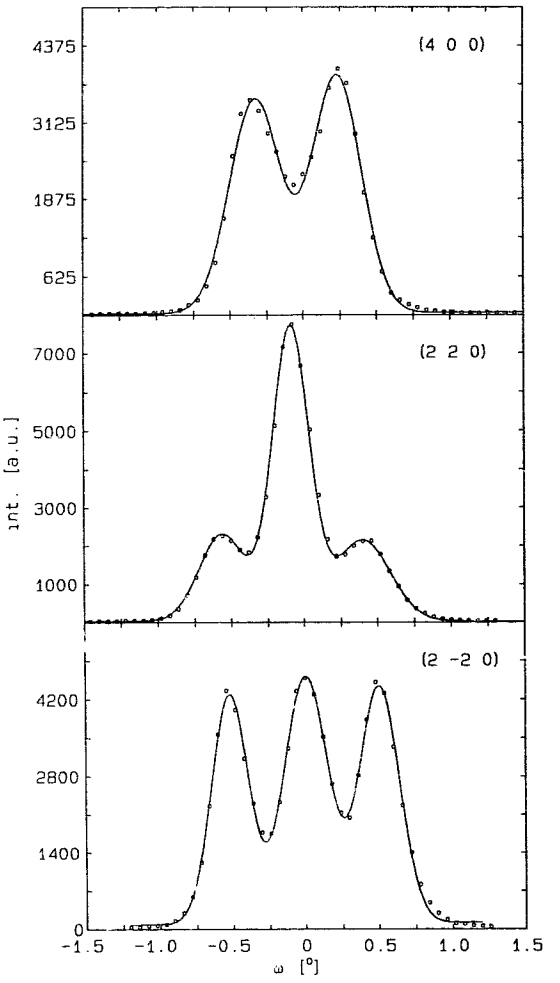

Fig. 3. Intensity profiles of the (400), (220) and (2 −20) Bragg reflections of the $La_2CuO_{4.005}$ crystal in the ω-scan mode with the c-axis perpendicular to the diffraction plane.

central peak is only as high as each of the two satellites, which show equal intensity, whereas for (220) the intensity of the central peak is about four times larger than those of the satellites. The sum of the three contributions is equal at (220) and (2 −20). Furthermore, the two peaks at (040) do not have the same intensity.

For these crystals the volume parts of the two domain orientations sharing a (110) plane are almost equal, as the satellites of (hh0) have always nearly the same intensity. However in the second crystal as well as in other samples the ratio of the volumes of $Abma_1$ and $Abma_2$ domains are different. Using electron diffraction on small single crystalline grains it has been shown that the twins form sets of lamellae of platelike domains parallel to (110) or (1 −10) with a typical thickness of the order of 1000 Å (for $YBa_2Cu_3O_{7-x}$ (123) see ref. [24], for $La_{2-x}Sr_xCuO_4$ [25]). The entire grain consists of lamellae sets of a size from several μm up to the order 10 μm, which contain a large amount of real monodomains. Each lamellae set contains only the two

orientations which are connected by the mirror plane ((1 1 0) or (−1 1 0)), to which the lamellae are parallel. The probability to find, within a finite sample volume, equal volume fractions of two orientations related by such a mirror plane is much greater than that to observe equal volume fraction of two different systems. This agrees with our findings that, say, $Abma_1$, and $Bmab_1$ are present by about the same amount but $Abma_1$ and $Abma_2$ are not.

We further examined two Sr doped crystals, with $x=0.07$ and $x=0.13$. In the less doped crystal we do not observe a comparable splitting of the profiles. But we still can prove the orthorhombicity at room temperature by centering a set of superstructure reflections which are forbidden in the tetragonal spacegroup. In fig. 4 we show the scans at the (2 2 0) nd (0 0 14) reflections. The peakwidth of the (0 0 14) reflection is increased by 0.11(3)° with respect to the experimental resolution, indicating that the stacking of the different CuO planes is less perfect in this crystal. We fitted the ($hk0$) profiles with a simple Gaussian function, but the results were not satisfying. The FWHM varies from 0.40(2)° at (0 0 14) and 0.45(2)° at (0 4 0) to 0.49(2)° at (2 2 0), indicating that the peak splitting observed in the undoped samples is reduced here to a peak broadening. A significant improvement is only achieved by introducing an additional central component on the tetragonal position of the lattice. In all fits the FWHM of the additional peak converges to about 0.7°, giving a contribution of about 5% to the entire intensity. The origin of this relatively broad component is still unclear. It is probably due to the poorer quality and/or special microstructure of this sample. Several explanations seem to be possible: a limited homogeneousness of the Sr distribution with its influence on T_{T-O} may yield remaining small tetragonal regions of higher Sr concentrations. Small orthorhombic domains may cause broadened peaks whose superposition may not be distinguished from a central component. In this case the higher amount of twin boundaries can further lead to a direct influence of the strain field associated to the boundaries. In regions, where all domains are very small, the superposition may be coherent, which would lead to an averaged tetragonal lattice, as has been observed in $YBa_2Cu_{3-x}Fe_xO_7$ [26]. It is important to underline that this finding cannot be related to the Sr doping, as it is not observed in the higher doped very perfect crystal $La_{1.87}Sr_{.13}CuO_4$ at low temperatures in the LTO phase.

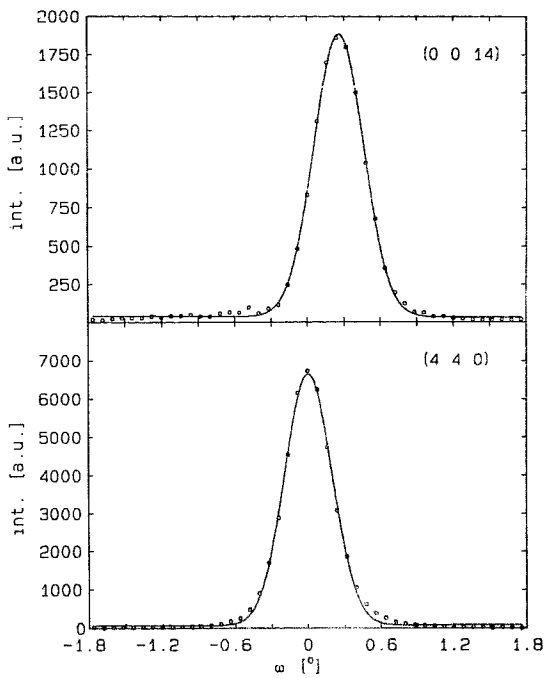

Fig. 4. Intensity profiles of the (0 0 14) and (2 2 0) Bragg reflections of the $La_{1.93}Sr_{0.07}CuO_4$ crystal in the ω-scan mode with the c-axis perpendicular to the diffraction plane.

If we compare the twinning conditions in the La_2CuO_4 system with those for 123 compounds, we find an important difference. In 123 compounds the orthorhombic basis a, b is equivalent to one mesh of the CuO_2 network. The twinning symmetry elements are again the (1 1 0) or (1 −1 0) planes, but they are oriented along the diagonals of the Cu–O squares, whereas in La_2CuO_4 these planes are parallel to the sides of the squares. Furthermore, the orthorhombic distortion is quite different. Therefore, twin boundaries in these two systems may have rather different effects on different physical properties, especially on the flux pinning [27].

Our results of the profile analyses on $La_{2-x}Sr_xCuO_4$ crystals are quite similar to those obtained on a large number of 123-crystals [31]. Usually almost equal volume fractions of the twin orientations have been found in the examined 123-crystals. Only very re-

cently deviations from an equal distribution have been observed in 123-crystals of high quality [31]. In crystals having equal volume fractions of the differently oriented domains the mosaic spread of the single components has always been relatively large, hence we conclude that in both systems the deviation is only possible in crystals of good quality. With the results of the electron diffraction this indicates that in such crystals the lamellae sets can become quite large, whereas crystal defects seem to reduce the size of the sets. Probably lattice defects act as pinning centers for the twin boundaries, especially for those between domains belonging to different lamellae sets.

3.2. Influence of the microstructure on the extinction

We further examined on these different crystals the influence of the microstructure on the extinction. ω-scans haven been recorded of a certain $(h\,k\,l)$ reflection for different orientations of the crystal in turning it around its reciprocal lattice vector [h k l]. As an example, we show in fig. 5 results for three crystals; Ψ is the angle between the current orientation and the bisecting one. The integrated ω-scan intensity of the (0 0 6) reflection of both $La_2CuO_{4+\delta}$ crystals show quite sharp minima, whereas the intensities of the (1 1 5) and (0 0 6) reflections of $La_{1.93}Sr_{0.07}CuO_4$ are almost independent of Ψ. The minimum intensity of La_2CuO_4 (fig. 5(a)) is about 25% less than at the plateau. For the (0 0 14) reflection we find a similar behaviour with much flatter minima.

As absorption effects in these samples are only very weak (the linear absorption coefficient $\mu \sim 0.1\ cm^{-1}$) the intensity behaviour of the Ψ-scans shown in fig. 5 must be due to anisotropic extinction effects. The observed minima can be completely understood considering the microtwinning. It is well known that a phase transition can change extinction conditions drastically, even if it is of second order. The very structured extinction in the case of our crystals reflect therefore the orientation of the domain boundaries. By turning the sample around the scattering vector [0 0 6], or the c-axis, there will be Ψ-angles, at which the (1 1 0) or the (1 −1 0) planes are parallel to the diffraction plane. The main feature in the

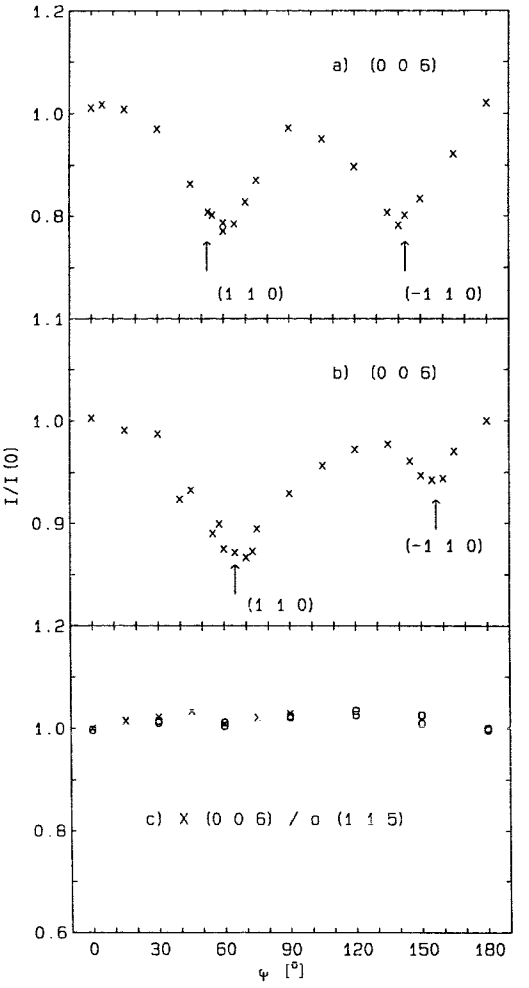

Fig. 5. Integrated intensity of a Bragg reflection as a function of the Ψ-angle (a) (0 0 6) for La_2CuO_4, (b) (0 0 6) for $La_2CuO_{4.005}$, (c) (0 0 6) and (1 1 5) for $La_{1.93}Sr_{0.07}CuO_4$ – the positions with the twin lamellae parallel to the diffraction plane are indicated by arrows.

$I(\Psi)$-curves is the loss of intensity for Ψ values near to these special orientations. As mentioned above the twin domains have a platelike shape parallel to the (1 1 0) or (1 −1 0) planes. If the diffraction plane is oriented just parallel, the neutron beam will stay in a single domain without passing several domain boundaries. So, the primary and secondary extinction, not limited by small domain sizes, cause the observed intensity loss. The effect at Ψ values with (1 1 0) or (1 −1 0) planes parallel to the diffraction

plane is almost the same, as is expected due to the similar volume fractions of the two sets $Abma_1$/$Bmab_1$ and $Abma_2$/$Bmab_2$. A detailed knowledge of such strong extinction anomalies is of great importance for quantitative intensity measurements. As a consequence of the rectangular shape of our La_2CuO_4 crystal, the angle between the intensity minima is not exactly equal to 90° and their positions coincide not exactly with the twin boundaries parallel to the diffraction plane.

In the $La_2CuO_{4.005}$ crystal (fig. 5(b)) we observed a similar behaviour with flatter minima at positions where the (1 1 0) planes are exactly parallel to the diffraction plane. As is shown in fig. 3 the fractions of the four different orientations are not similar. The volume fractions of the two orientations with a common (1 1 0) plane is about two times larger than that of the other set. This is reflected in the extinction behaviour by the deeper minimum at the position where (1 1 0) is parallel to the diffraction plane. Furthermore, the extinction effect is reduced with respect to the first crystal, which is attributed to smaller domain sizes.

The only difference between these two crystals is an additional oxygen annealing of the second, which reduces the orthorhombic splitting and the antiferromagnetic transition temperature (see table 1). The additional oxygen seems to influence the microtwinning by causing a smaller average domain size. The excess oxygen may favour the formation of twin boundaries as other impurities do [28], or may even be located in the twin boundary.

In fig. 5(c) we show the Ψ-scan results of the Sr doped crystal, where no comparable intensity minima can be found. The mosaicity of this crystal is larger, which already explains smaller extinction effects. In agreement with the broadened Bragg reflections, strongly reduced domain sizes may further reduce the conditions for extinction.

3.3. Temperature dependence of the domain structure

The observed extinction effects offer the possibility to study the formation of the twinning at the HTT–LTO transition. In fig. 6 we show the integrated intensity of the (2 2 0) reflection of the $La_{1.87}Sr_{0.13}CuO_4$ crystal (T_{T-O} = 196.5 K) as a function of temperature. Due to the good quality of the crystal, extinction effects are very strong in the tetragonal phase. At room temperature the intensity is reduced by about 80% as determined by a structure refinement [29]. Below the phase transition the intensity increases strongly as the extinction becomes less important due to the formation of the twinning domains. It is astonishing that this effect is not smooth, as could be expected for a second order phase transition, but shows a steplike behaviour. The formation of the twins occurs just at the critical temperature T_{T-O}. In the orthorhombic phase the microstructure characterized by the domain sizes and their distribution is fixed. The slope of the intensity versus temperature curve above and below the phase transition is almost equal and is mainly due to the Debye–Waller factor. With decreasing temperature the orthorhombic strain is strongly enhanced, thus increasing the energy for the domain boundaries. We first cooled the $La_{1.87}Sr_{0.13}CuO_4$ crystal and measured the intensity only at a few temperatures, then we measured the complete temperature dependence of fig. 6 on heating. No difference between the intensities on cooling and on heating was found, but it is important to note that this crystal had already been cooled to the LTO phase before our experiment. This indicates that the formation of the twinning domains is reversible at least after several cooling cycles, and that the quality of the HTT lattice after cooling is not affected by the orthorhombic distortion or the twinning at low temperatures. We further studied the reversibility of the volume distribution of the orien-

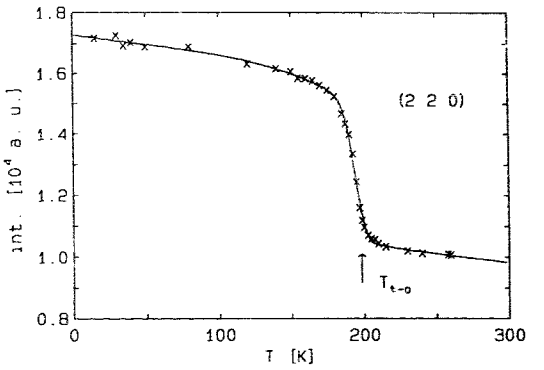

Fig. 6. Temperature dependence of the integrated intensity of the (2 2 0) Bragg reflection of the $La_{1.87}Sr_{0.13}CuO_4$ crystal.

tations with this crystal at low temperatures. For this purpose we used a triple axis spectrometer (G4.3 at the reactor ORPHEE) in a high q-resolution configuration ($\lambda = 2.36$ Å, collimation 10'−10'−30'). At 50 K we determined the four volume fractions of $Abma_1$, $Bmab_1$, $Abma_2$ and $Bmab_2$ orientations with the scans described above to 47(2):47(2):3(2):3(2). Then the crystal stayed at room temperature well above the phase transition for several weeks. After this time we cooled for a second time and remeasured the volume fractions and found again the quite unusual values 45(2):45(2):5(2):5(2). In spite of the high uncertainties of these short experiments these results support clearly the reversibility of the microdomain structure of $La_{2-x}Sr_xCuO_4$ crystals.

In this context it is interesting to look at the geometrical conditions of the twin boundary. Figure 1(a) indicates that this boundary can be infinitely long as there is no mismatch which would increase proportional to its size. The energy of such a boundary divided by its area is constant. In addition to this type of boundary there are two other types, which separate two domains of different sets of lamellae. $Abma_1$ and $Bmab_2$ domains are connected by a 90° rotation around [001]. At the corresponding boundary the long orthorhombic axis of one twin is parallel to the short one of the second. The magnitude of the misfit between two lattices in neighbouring domains increases with the length of the boundary, at $a/(a-b)$ cells it amounts to one cell parameter. As a consequence this boundary cannot become much larger than about $0.2a/(a-b)$ cells without a strong and therefore irreversible distortion of the lattice. Furthermore, the energy of such a boundary increases drastically with the orthorhombic strain. For the third type of boundaries between $Abma_1$ and $Abma_2$ domains the misfit increases with its length, as it is caused by the tilting Δ between their orientations. It is therefore reasonable to assume that only the first type of boundary (shown in fig. 1(a)) causes no strong lattice defects and that it can become very extended. This is in agreement with the lamellae structure of the domains observed by electron microscopy [25].

These arguments support the following picture of the formation of the twin structure during the phase transition. If the crystal is cooled the first time to the LTO phase, the evolving twin structure is only influenced by the defects of the HTT phase. As the boundaries of the second and third type cause large strains, it will be favourable to avoid them by developing large sets of lamellae. But the already existing crystal defects may force the crystal to form different sets of lamellae and therefore to form also the "high strain" boundaries. There the lattice is strongly distorted, either as a consequence of the twinning which creates new defects or due to old defects of the HTT phase, which pin the boundary. But the first cooling seems not to produce a lot of very strong defects, as the HTT phase in the $La_{1.87}Sr_{0.13}CuO_4$ crystal shows a very high quality after reheating. We can therefore conclude that the size of the "high strain" boundaries is not much higher than $a^2/(a-b)$. If the crystal is cooled for a second time to the LTO phase, it will reestablish the same domain structure due to the defects which existed before the first cooling and due to the defects which were caused or deplaced by the domain structure during the first cooling. The formation of the domains is now reversible, as has been observed in our measurement. In isolated grains of 123 a narrowing of the twin spacing has been observed at low temperatures [30], which did not occur in grains in close contact to each other. Our measurements indicate that this behaviour does not exist in the $La_{1.87}Sr_{0.13}CuO_4$ crystal, at least not down to 20 K. As in our case the orthorhombic distortion increases even stronger on decreasing temperature, which leads to higher strains at the twin boundaries especially between the lamellae sets, it should be favorable to reduce the average twin size at low temperatures. Probably the pinning of the domain structure by defects prevents such a refinement in the single crystal and in grains with close contact. Therefore, there may be an influence of the specific domain structure on the phase transition with respect to a monodomain system or a free grain. This influence will increase with the amount of the "high strain" twin boundaries between two lamellae sets, and therefore with the amount of defects.

3.4. Structure analysis

During the structure investigation of $La_{1.93}Sr_{0.07}CuO_4$ in the LTO phase at room temper-

ature we studied the extinction rules for systematic absent reflections according to the superposition of the Abma and Bmab lattices. Only a few sharp forbidden reflections (e.g. (5 0 0) and (3 0 3)) were found to have significant intensities after correction for $\lambda/2$ contamination. By improved statistics we proved that all these intensities are smaller than 0.1% of the intensity of the strongest reflection. As we never could observe a complete set of equivalent forbidden reflections, the small peaks are probably due to multiple diffraction. In addition we find large peaks (FWHM $\sim 2°$) with significant intensities at some (0 0 l) positions (with l=odd, especially (0 0 7) and (0 0 11)). These are observed in other $La_{2-x}Sr_xCuO_4$ crystals too and are not understood up to now.

3687 reflections have been measured of which 1460 are independent. The internal R-value from the averaging in the Laue class mmm amounts to 1.8% for the entire set proving the good quality of the data including the complete integration of the multi-peak intensity profiles. As the crystal has nearly the shape of a cube and the absorption coefficient is very small ($\mu \sim 0.1$ cm^{-1}) no absorption correction has been performed.

In the refinements we used only the set of 958 reflections which are allowed by the superposition of Abma and Bmab lattices. The exploitation of the superimposed intensities has to take into account the twinning. The two Abma ($Abma_1$ and $Abma_2$) and the two Bmab ($Bmab_1$ and $Bmab_2$) domain orientations need not be distinguished in the intensity treatment. Only the ratio between the Abma and the Bmab parts is important. The observed intensity is the sum of these two contributions [32]:

$$I^{\mathrm{obs}}_{hkl} \propto \alpha F^2_{hkl} + (1-\alpha) F^2_{khl}\,, \qquad (2)$$

where α is the volume fraction of the two Abma orientations and F_{hkl} and F_{khl} are the structure factors in Abma symmetry.

By comparing the intensities of superstructure reflections ($h\,k\,l$) with $h+l$ odd ($F_{khl}=0$, $F_{hkl}\neq 0$) with those of ($k\,h\,l$) we obtain directly the volume fraction $\alpha = 50.8(2)\%$. These two reflections are not independent; they are related by

$$I(hkl) = \frac{\alpha}{1-\alpha} I(khl)\,. \qquad (3)$$

According to this relation the number of independent reflections is further reduced to 661 of which 585 are stronger than $2.5\sigma(I)$.

The data are refined using a version of the Prometheus program package, which had been modified for a treatment of twinned crystals [33]. The volume fraction α was kept fixed to the value obtained from the intensity ratio of corresponding superstructure reflections. As extinction effects in this crystal are small but not negligible, corrections according to the Becker and Coppens formalism for secondary extinction of type I assuming a Lorentzian distribution [33] were applied. We allowed for the variation of the occupation probabilities of the La, O(1) and O(2) sites, all the free positional and the anisotropic thermal parameters starting with the values given in ref. [6]. There were strong correlations between U_{11} and U_{22} for O(1) as well as for Cu, so we constrained $U_{11}=U_{22}$ for these two sites without a significant consequence for the R-values and obtained $R_w(F^2)=0.029$ and $R(F^2)=0.021$. Due to the two-dimensional character of the La_2CuO_4-structure, it was reasonable to assume a simple anisotropic extinction model. Only two independent extinction parameters $G_{11}=G_{22}$ and G_{33} corresponding to the components of the neutron path parallel and perpendicular to the CuO_2 plane were included. The specific mounting of the crystal allows us to continue the refinement with the averaged data set even in the case of anisotropic extinction, as all symmetry equivalent reflections have been measured with the same angle between c-axis and diffraction plane. With only one additional extinction parameter we obtain an improvement of the R-values to $R_w(F^2)=0.026$ and $R(F^2)=0.019$.

As multiple diffraction and thermal diffuse scattering can lead to an overestimation of the intensity of weak reflections we tried to reduce their importance in the structure refinement in modifying our weighting scheme $1/\sigma(F^2)$:

$$\sigma_{\mathrm{new}} = \sqrt{\sigma^2_{\mathrm{old}} + \mathrm{const.}^2} \qquad (4)$$

with const. = 2.5. Using the altered weighting scheme we obtain improved R-values $R_w(F^2)=0.0175$ and $R(F^2)=0.0183$, indicating that weak reflections may be affected. The final weighting scheme leads to only small changes in the structural parameters, but the amount of vacancies on the La and the O sites is re-

duced by about 5σ. Furthermore the difference between U_{11} and U_{22} of the La site turns out to be insignificant. Therefore we constrained also $U_{11}=U_{22}$ for the La site (without influence on the R-value) and got the final results, which are shown in table 2 and in the form of an ORTEP plot in fig. 7. There we show only the atom sites of the smaller I4/mmm unit cell, as the whole presentation of the Abma cell renders the picture less clear. Due to the correlation of the weighting scheme and the occupation probabilities the latter remain doubtfull: O(1) 0.995(3), O(2) 1.002(3) and La 0.981(3) (the error values are obtained by the fit). There seems to be a significant amount of vacancies at the La/Sr site. The refined occupation probability corresponds to a Sr concentration $x=0.22$ (in $La_{2-x}Sr_xCuO_{4+\delta}$). This

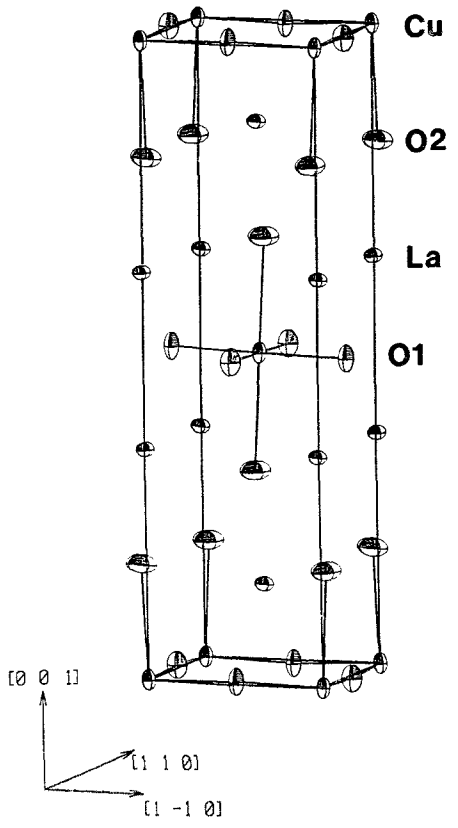

Fig. 7. ORTEP plot of the room temperature LTO structure of $La_{1.93}Sr_{0.07}CuO_4$. Only the atom sites of the I4/mmm unit cell are displayed. The thermal ellipsoids correspond to the 85% occupation probability.

Sr concentration is in clear disagreement with the lattice constants and the transition temperature T_{T-O} [21]. Therefore, we conclude that the real Sr concentration is close to $x=0.07$ and that there are $\sim 1\%$ vacancies at this site. This and the other structural parameters will be discussed together with results obtained on other crystals in a forthcoming publication.

3.5. Comparison of different structural models

After the refinement of the data set it is still not certain, that the applied refinement procedure yields the correct solution, and that the tetragonal space group $P4_2/ncm$ can be excluded. Hence we attempted to clarify this point by further calculations. The STOE program package of the P110 diffractometer has been used to calculate a set of synthetic structure factors for the untwinned Abma structure, which were free of statistical errors. As atomic positional and thermal parameters we used the values from the structure refinement of $La_{1.93}Sr_{.07}CuO_4$, which are shown in table 2. First the squares of the structure factors were coupled to the twinned case using eq. (2) and assuming a volume fraction of 60% Abma and 40% Bmab orientations. If we treat the artificial data set in the Abma space group assuming a monodomain untwinned structure there are a lot for forbidden but strong reflections due to the Bmab oriented parts. Furthermore, the refinement yields displacement parameters x(La), z(O(1)) and x(O(2)) which are significantly too small, and some unreasonable thermal parameters. In this model the Abma specific reflections are strongly overestimated as the input Abma fraction of 60% is set in the Abma model to 100%. Using the modified refinement procedure, which takes twinning into account, we obtain the expected parameters within the numerical errors ($R(F)=0.0003$). The refinement converges very fast without any indication of other minima in spite of anticipated complications due to twinning. However, the twinning causes correlations between U_{11} and U_{22} for the La, Cu and O(1) sites similar to the experimental observations. We further checked the influence of errors of the volume fraction parameter α on the refinement results. By assuming a volume fraction of $\alpha=0.605$ we found only small changes in the R value and in the resulting param-

eters, which would be insignificant in an experiment.

The refinement of the artificial data with the tetragonal space group $P4_2/ncm$ led to the surprisingly good R factor of $R(F)=0.0059$. But as the chosen volume ratio differs significantly from 50:50, there are a lot of inconsistencies in the data reduction procedure, which averages the symmetrical equivalent reflections, leading to a bad R_{int} value. The tetragonal symmetry can be already excluded by these inconsistencies. In order to further examine the possible application of the $P4_2/ncm$ space group, we calculated a second artificial data set according to eq. (2) and the ideal twinning ratio of $\alpha=50\%$. Again we could refine this set with the modified refinement procedure within the numerical errors. The refinement using the $P4_2/ncm$ spacegroup fits this set better than the first one, leading to $R(F)=0.0037$. Like the LTO phase of La_2CuO_4 the tetragonal modification of space group $P4_2/ncm$ phase is derived from the HTT K_2NiF_4 structure by a tilt of the CuO_6 octahedra. In the case of the LTO phase this tilt is around a [1 0 0] direction, in space group $P4_2/ncm$ it is around the [1 1 0] direction (in the orthorhombic notation). In Abma the x coordinate of the O(2) site is one of the parameters which are significant for the lattice distortion, in $P4_2/ncm$ this corresponds to the $x=y$ parameter describing the displacement along [1 1 0]. The resulting deviation of the O(2) site from the c-axis ($x\times a$ in Abma) has to be compared to ($\sqrt{2}x\times a$) in $P4_2/ncm$. If we consider this, in both refinements of data set II the same distances to the tetragonal positions are obtained. A similar behaviour is found for the other relevant positions x(La) and z(O(1)). The refinements with the two different models lead to the same amplitudes of the tilt which differ only in their rotation axis. As the difference in the calculated R-value is very small, it is expected that it cannot be observed experimentally. In these cases it is important to obtain additional information about the orthorhombicity of such a crystal by the characteristic scans described above. One has to be extremely careful in the interpretation of integrated intensities for small orthorhombic strains. For the discussion of the sequence of phase transitions in $La_{2-x}Ba_xCuO_4$ this means that the intensities can determine the amplitude of the tilt of the CuO_6 octahedra but not the direction of the rotation axis.

Another interesting aspect was a possible coherent superposition due to very small domain sizes. Instead of a superposition of the intensities we have to add the structure factors:

$$F_{cal}=F_{Abma}+F_{Bmab}\,. \tag{5}$$

Even by assuming this model the refinement led to satisfying results, the obtained R factor is 0.0025 and the agreement of the positional and thermal parameters is good. The differences between F_{Abma} and F_{Bmab} seem to be too small to distinguish between the two kinds of superposition. Therefore a small amount of pseudotetragonal regions where coherent superposition may be present cannot change the obtained structural results. This further shows that it is almost impossible to distinguish between a pseudotetragonal structure due to microtwinning and the $P4_2/ncm$ space group only by an intensity analysis (on powders or on single crystals).

A similar discussion has been given for 123 compounds by Hönle et al. [34]. They examined the possibility of a distinction between statistical occupation of the chain oxygen sites and an orthorhombic microtwinning with incoherent superposition using single crystal X-ray diffraction. They concluded, that this would not be possible. The corresponding statistical model in the case of $La_{2-x}Sr_xCuO_4$ is a tetragonal structure with four-fold splitted La and O(2) positions at ($\pm x$, 0, z) and (0, $\pm y$, z) with an occupation probability of 0.25 and a two-fold splitted O(1) position (0.25, 0.25, $\pm z$) with an occupation probability of 0.5 (all parameters in the LTO notation). The symmetry of this structure is I4/mmm. This model is obviously ruled out by the presence of the super lattice reflections in the LTO phase. However for the 123 compounds too, we find using the scattering factors for neutron diffraction, that the statistical model can easily be distinguished by the analysis of certain reflections which are sensitive to the chain oxygen (e.g. (1 0 2)).

Acknowledgements

We wish to thank B. Winkler for several discussions and critical reading of the manuscript. We also

wish to thank S. Jungk, N. Knauf and W. Schnelle for the characterizing measurements.

References

[1] K.K. Singh, P. Ganguly and J.B. Goodenough, J. Solid State Chem. 52 (1984) 254;
A. Manthiram and J.B. Goodenough, J. Solid State Chem. 87 (1990) 402.
[2] D.I. Khomskii and K.I. Kugel, Solid State Commun. 13 (1973) 763;
R. Haegerle and D. Babel, Z. anorg. allg. Chemie 409 (1974) 11.
[3] J.M. Longoh and P.M. Raccah, J. Solid State Chem. 6 (1973) 526.
[4] D.C. Johnston, J.P. Stokes, D.P. Goshorn and J.T. Lewandowski, Phys. Rev. B 36 (1987) 4007.
[5] G. Demazeau, F. Tresse, Th. Plante, B. Chevalier, J. Etourneau, C. Michel, M. Hervieu, B. Raveau, P. Lejay, A. Sulpice and R. Tournier, Physica C 153–155 (1988) 824.
[6] R.M. Flemming, B. Batlogg, R.J. Cava and E.A. Rietman, Phys. Rev. B 35 (1987) 7191.
[7] R.J. Cava, A. Santoro, D.W. Johnson Jr. and W.W. Rhodes, Phys. Rev. B 35 (1987) 6716.
[8] M. Francois, K. Yvon, P. Fischer and M. Decroux, Solid State Commun. 63 (1987) 35.
[9] D.T. Keane, G.A. Held, J.L. Jordan-Sweet, M.W. Shafer, P.M. Horn, G. Günherodt, J. Langen, M. Weit, A. Erle, S. Blumenröder and E. Zirngiebl, Physica C 153–155 (1988) 594.
[10] J.D. Axe, A.H. Moudden, D. Hohlwein, D.E. Cox, K.M. Mohanty, A.R. Moodenbaugh and Youwen Xu, Phys. Rev. Lett. 62 (1989) 2751.
[11] T. Suzuki and T. Fujita, Physica C 159 (1989) 111.
[12] S.W. Cheong, J.D. Thompson and Z. Fisk, Physica C 158 (1989) 109.
[13] I. Takayama, Jpn. J. Appl. Phys. 27 (1988) L2283.
[14] P. Galez, P. Schweiss, G. Collin and R. Bellissent, J. Less-Comm. Met. 164–165 (1990) 784.
[15] B. Büchner, M. Braden, M. Cramm, W. Schlabitz, W. Schnelle, O. Hoffels, W. Braunisch, R. Müller, G. Heger and D. Wohlleben, Proc. M²-HTSC III, Physica C 185–189 (1991) 903.
[16] R.J. Birgeneau, C.Y. Chen, D.R. Gabbe, H.P. Jensen, M.A. Kastner, C.J. Peters, P.J. Picone, Tineke Thio, T.R. Thurston and H.L. Tuller, Phys. Rev. Lett. 59 (1987) 1329.
[17] S.V. Malleyev and B. Toperverg, Solid State Commun. 67 (1988) 405.
[18] H. Schmid, E. Burkhardt, Bing Nan Sun and J.P. Rivera, Physica C 157 (1989) 555.
[19] I. Tanaka and H. Kojima, Nature 337 (1989) 21.
[20] S.W. Cheong, J.D. Thompson and Z. Fisk, Phys. Rev. B 39 (1989) 4395.
[21] H. Takagi, T. Ido, S. Ishibashi, M. Uota, S. Uchida and Y. Tokura, Phys. Rev. B 40 (1989) 2254.
[22] G. Friedel, Lecons de cristallographie, 1926 Paris: Berger Levrault, reprinted 1964 Paris: Blanchard.
[23] J.M. Delgado, R.K. McKullan, G. Diaz de Delgado, B.J. Wuensch, P.J. Picone, H.P. Jenssen and D.R. Gabbe, Phys. Rev. B 37 (1988) 9343.
[24] G. Roth, D. Ewert, G. Heger, M. Hervieu, C. Michel, B. Raveau, F. D'Yvoire and A. Revcolevschi, Z. Phys. B: Cond. Matt. 69 (1987) 21.
[25] C.H. Chen, S.W. Cheong, D.J. Werder, A.S. Cooper and L.W. Rupp, Physica C 175 (1991) 301.
[26] G. Roth, G. Heger, B. Renker, J. Pannetier, V. Caignaert, M. Hervieu and B. Raveau, Z. PHys. B: Cond. Matt. 71 (1988) 43.
[27] W.K. Kwok, U. Welp, G.W. Grabtree, K.G. Vandervoort, R. Hulscher and J. Z. Liu, Phys. Rev. Lett. 64 (1991) 966.
[28] W.W. Schmahl, A. Putnis, E. Salje, P. Freeman, A. Graeme-Barber, R. Jones, K.K. Singh, J. Blunt, P.P. Edwards, J. Loram and K. Mirza, Philos. Mag. Lett. 60 (1989) 241.
[29] M. Braden, unpublished data.
[30] J.F. Smith and D. Wohlleben, Z. Phys. B: Cond. Matt. 72 (1988) 323.
[31] P. Schweiss, unpublished data, recent measurements on 123-single crystals prepared by A. Erb, Univ. Karlsruhe.
[32] C. Chaillout, S.W. Cheong, Z. Fisk, M.S. Lehmann, M. Marezio, B. Morosin and J.E. Schirber, Physica C 158 (1989) 183.
[33] U.H. Zucker, E. Perenthaler, W.F. Kuhs, R. Bachmann and H. Schulz, J. Appl. Crystallogr. 16 (1983) 358;
A. Belzner, unpublished Ph. D. thesis, Ludwig-Maximilians Universität, München, 1988.
[34] W. Hönle and H.G. von Schnering, Z. Kristallogr. 184 (1988) 301.